NUWC-NPT Technical Document 10,479
30 September 1993

Flextensional Transducer Modeling Using Variational Principles

Presented at the 124th Meeting of the Acoustical Society of America, New Orleans, Louisiana, November 1992

H. C. Robinson
Environmental and Tactical Support Systems Department

R. T. Richards
J. B. Blottman III
Submarine Sonar Department

Naval Undersea Warfare Center Division
Newport, Rhode Island

PREFACE

This work was supported by the NUWC Independent Research/Independent Exploratory Development (IR/IED) Program and was presented at the 124th meeting of the Acoustical Society of America, November 1992, in New Orleans, Louisiana.

Reviewed and Approved: 30 September 1993

F. V. Kingsbury

F. J. Kingsbury
Head: Submarine Sonar Department

B. F. Cole

B. F. Cole
Head: Environmental and Tactical Support Systems Department

REPORT DOCUMENTATION PAGE

Form Approved
OMB No. 0704-0188

1. AGENCY USE ONLY (Leave Blank)	2. REPORT DATE	3. REPORT TYPE AND DATES COVERED
	30 September 1993	Final

4. TITLE AND SUBTITLE

Flextensional Transducer Modeling Using Variational Principles

5. FUNDING NUMBERS

PR A63400

6. AUTHOR(S)

H. C. Robinson, R. T. Richards, and J. B. Blottman III

7. PERFORMING ORGANIZATION NAME(S) AND ADDRESS(ES)

Naval Undersea Warfare Center Detachment
39 Smith Street
New London, Connecticut 06320-5594

8. PERFORMING ORGANIZATION REPORT NUMBER

TD 10,479

9. SPONSORING/MONITORING AGENCY NAME(S) AND ADDRESS(ES)

Naval Undersea Warfare Center Division
1176 Howell Street
Newport, RI 02841-1708

10. SPONSORING/MONITORING AGENCY REPORT NUMBER

11. SUPPLEMENTARY NOTES

Presented at the 124th Meeting of the Acoustical Society of America, New Orleans, Louisiana, November 1992.

12a. DISTRIBUTION/AVAILABILITY STATEMENT

Approved for public release; distribution is unlimited.

12b. DISTRIBUTION CODE

13. ABSTRACT (Maximum 200 words)

This document contains the presentation entitled "Flextensional Transducer Modeling Using Variational Principles" given at the 124th meeting of the Acoustical Society of America.

14. SUBJECT TERMS
Flexural Transducer Modeling

15. NUMBER OF PAGES
16

16. PRICE CODE

17. SECURITY CLASSIFICATION OF REPORT	18. SECURITY CLASSIFICATION OF THIS PAGE	19. SECURITY CLASSIFICATION OF ABSTRACT	20. LIMITATION OF ABSTRACT
Unclassified	Unclassified	Unclassified	SAR

FLEXTENSIONAL TRANSDUCER MODELING USING VARIATIONAL PRINCIPLES

INTRODUCTION

Variational principles are an approximation method that allows one to obtain accurate estimates for a quantity of interest using relatively crude representations, known as trial functions, for the physical behavior of the system. This method is applied to flextensional transducer analysis by coupling a variational principle developed for the resonance frequency of the piezoelectric driving element to one for the resonance frequency of the shell, carefully ensuring that the boundary conditions at the driver-shell interface are satisfied. The *in-vacuo* mode shapes and resonance frequencies for a Class V ring-shell transducer calculated in this manner are compared with finite element modeling and experimental data for the first two modes of the transducer. There is excellent agreement between the methods in the calculation of the resonance frequencies, even though the mode shapes calculated variationally do not agree exactly with the finite element predictions.

Fluid-loading effects on the transducer are introduced by coupling the in-vacuo variational transducer model to a variational principle for the surface pressure of a radiating body based on the Helmholtz integral equation. The surface pressures determined using the variational formulation and the finite element method for a single Class V ring-shell projector are compared for the first two resonant modes. It is shown that the agreement for the surface pressure is better for the first mode, but in both cases the agreement is still reasonable. Explanations for these discrepancies are discussed. Options for calculating the far-field pressures from the variationally determined surface pressures are presented.

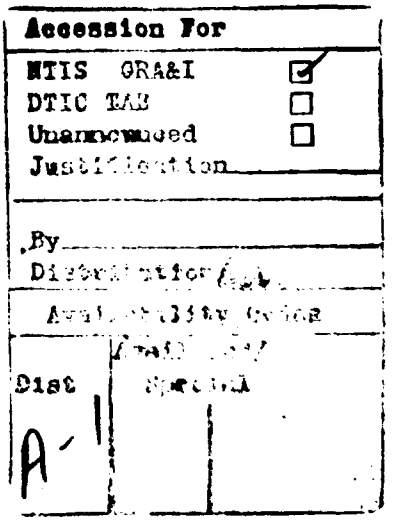

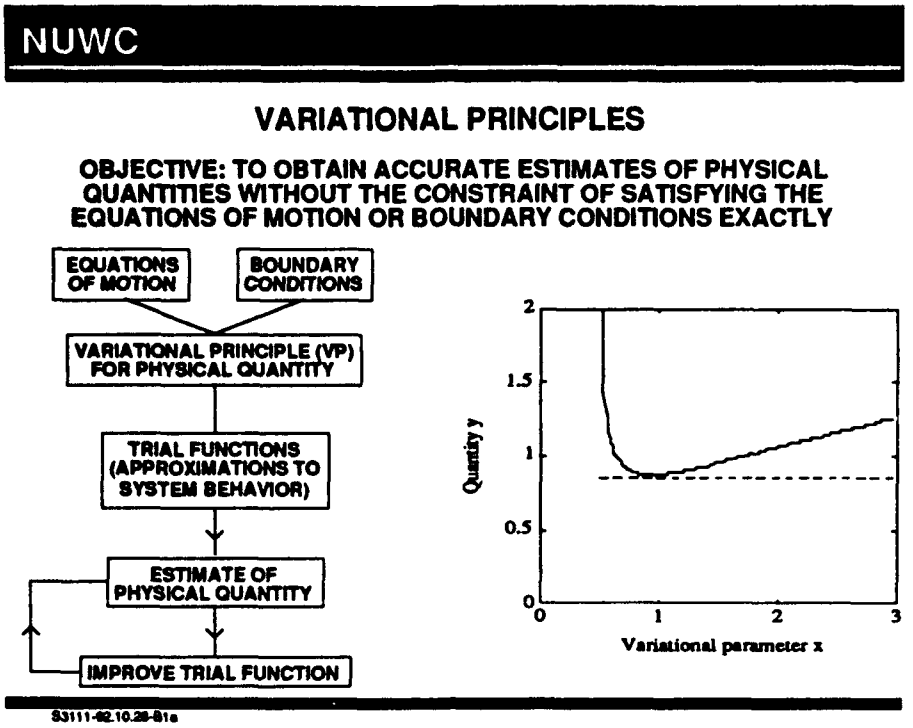

FIGURE 1

A variational principle (VP) provides estimates of a particular physical quantity without having to satisfy the equations of motion or the boundary conditions exactly. The equations of motion describing a particular system, along with the applicable boundary conditions, are combined using a generalized method given by E. Gerjuoy, A.R.P. Rau and L. Spruch [Rev. Mod. Phys. 55, pp. 725-774 (1983)] into a variational expression for some quantity of interest, say y. Approximations to the physical behavior of the system, known as trial functions, are then incorporated into the VP to yield the estimate. The accuracy of this estimate can be improved by improving the trial functions, either by incorporating more terms if using a basis function expansion (Rayleigh-Ritz method) or by allowing the trial functions to satisfy at least some of the boundary conditions. On the right hand side, this process is illustrated by assuming that the quantity y depends on some complicated function z of a parameter x. We denote the trial function by z_t=f(x), where f(x) is a relatively crude approximation to z, and vary x. The variational estimate of y is shown by the solid line, while the exact solution is the dotted line. The best estimate of y for the particular choice of trial function z_t occurs at some optimum value for x, at which the minimum occurs. About this optimum value, the variational curve is relatively flat, showing that the variational estimate is stationary with respect to small variations of x about this optimum value. The crude trial function z_t yielded a very accurate estimate of the quantity y, demonstrating that a variational estimate is always more accurate than the trial function used to obtain it.

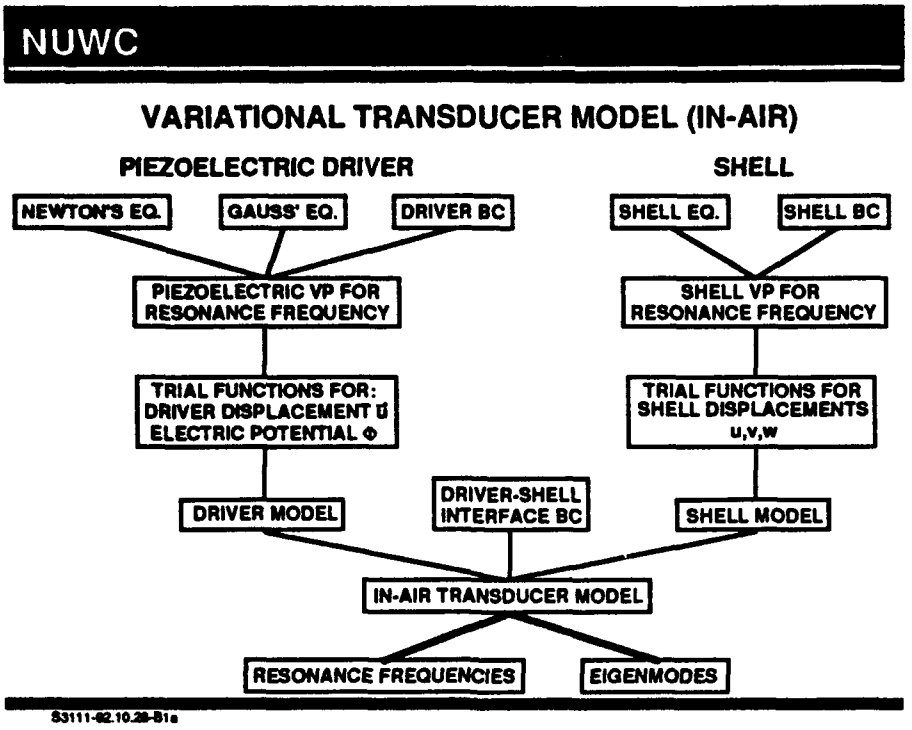

FIGURE 2

The derivation of a variational model for a *flextensional* transducer is illustrated by the flowchart above. The primary constituents of such a transducer are a driver, usually consisting of piezoelectric ceramic, attached to an elastic shell. The extensional motion of the driver causes the shell to move in a flexural mode, hence the term flextensional. To obtain a variational model for the transducer as a whole, variational expressions for the resonance frequency of the individual parts are derived. Newton's force equations and Gauss' law for the piezoelectric material, expressed in the notation of B.A. Auld [Acoustic Fields and Waves in Solids, Wiley-Interscience, New York (1973)], are combined with appropriate boundary conditions to yield a VP for the resonance frequency of the driver. The appropriated independent variables for this VP are the driver displacement $\vec{u}$ and the electric potential Φ. Similarly, shell equations, such as the generalized equations in A.W. Leissa ["Vibration of Shells," NASA Sp-288, Washington, D.C., 1973], and boundary conditions, e.g. free, clamped, etc., yield a VP in terms of the normal shell displacement w and two tangential displacements u and v. The models for the piezoelectric driver and spherical shell cap for a Class V ring-shell projector have been verified by the authors previously ["Variational Modeling of Class V Flextensional Ring-Shell Projectors," in Transducers for Sonics and Ultrasonics, Technomic, Lancaster, Pa., pp. 209-221 (1992)]. Once the individual VPs have been verified, they may be coupled, using interface boundary conditions, into a variational model for the transducer. This model will yield highly accurate estimates for the eigenfrequencies but gives less accurate mode shapes.

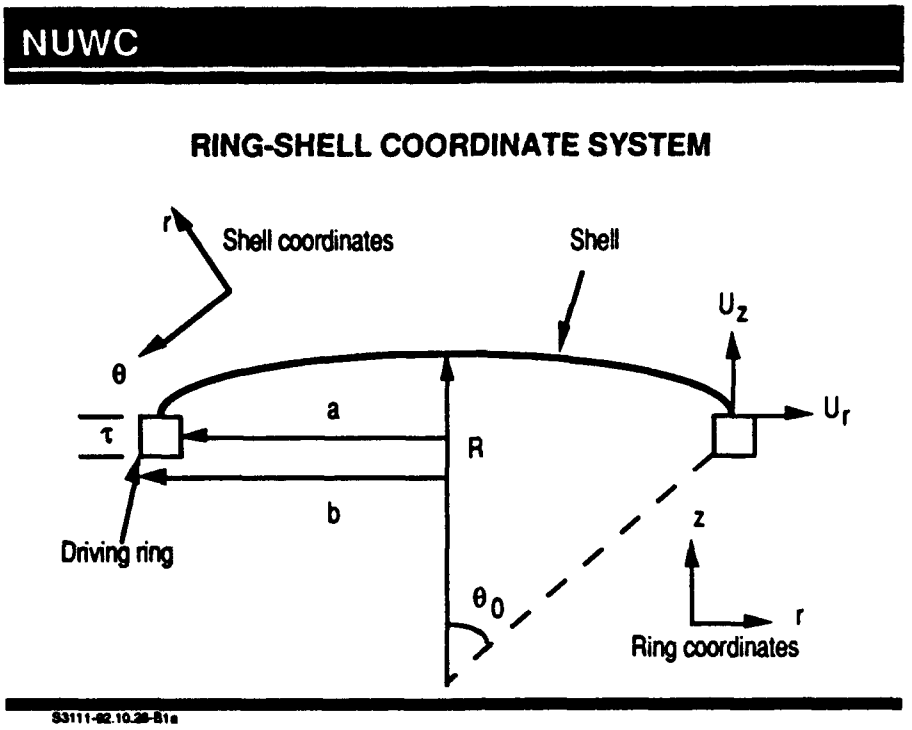

FIGURE 3

A cut-away diagram of the simplified ring-shell transducer configuration modeled is shown above. The driver consists of slabs of piezoelectric ceramic alternating with wedges of steel to form a ring. The ceramic is arranged such that the poling of the driver is tangential, and the net effect of the extension of the slabs produces radial motion in the ring. The driver has an inner radius a, outer radius b and a height τ The preferred coordinates for the ring are cylindrical coordinates (r,θ, z). Since the motion of the ring is axisymmetric, the driver displacements of consequence are the radial displacement u_r and the axial displacement u_z

Two spherical shell caps, typically composed of steel, are mounted to the top and bottom of the ring driver. The bottom shell is not shown here for simplicity. In the shell (spherical) coordinate system (r, θ, ϕ), the shell cap has a constant radius of curvature R and spans an azimuthal angle θ_0. The motion of the ring driver is transformed into flexural motion of the shell; since the driver motion is axisymmetric, only the normal shell displacement w and azimuthal displacement u are modeled.

It must be noted that several simplifications to the realistic ring-shell geometry have been made here. Most importantly, the shell is bolted to the ring driver via a flange. The effect of the flange will be modeled by matching the shell displacements and moments to those of the ring at the point of intersection. Furthermore, a fiberglass wrapping around the outside of the ring is neglected; the prestressing effect of this component will be accounted for by matching the normal stress on the outer ring radius to a nominal prestress value.

NUWC

TRIAL FUNCTIONS FOR RING DRIVER AND SHELL CAP

- **TRIAL FUNCTIONS FOR PIEZOELECTRIC RING DRIVER**

$$u_{rt} = \sum_{n=1}^{N_r} A_n [J_1(\lambda_n r) + B_n N_1(\lambda_n r)] \sin[(2q_n - 1)\pi z/\tau]$$

$$u_{zt} = \sum_{n=1}^{N_z} C_n [J_0(\eta_n r) + D_n N_0(\eta_n r)] \cos[(2p_n - 1)\pi z/\tau]$$

$$\Phi_t = \sum_{n=1}^{N_\phi} E_n \sin[\beta_n M\Theta/2]$$

- **TRIAL FUNCTIONS FOR SHELL DISPLACEMENT**

$$w_t = \sum_{n=0}^{N_s} W_n \cos(n\theta) \qquad u_t = \sum_{n=0}^{N_s} U_n \sin(n\theta)$$

S3111-92.10.28-81a

FIGURE 4

Modeling the ring in cylindrical coordinates (r, Θ, z), linear combinations of Bessel functions J_0 and J_1 and Neumann functions N_0 and N_1 are chosen as the basis for the driver displacements. The motion of the ring is essentially radial; however, z dependence is included to model the effects of higher order bending modes of the ring. The parameters η_n and λ_n, along with the coefficients B_n and D_n are determined so that stress-free boundary conditions on the inner and outer radii of the ring are satisfied. p_n and q_n are integers. Since the ring motion is axisymmetric, there is no dependence on the angle Θ for the displacement. However, since the ring is poled tangentially, the electric potential does depend on the angle but is assumed to constant with respect to the other dimensions of the ring. The factor M is simply the number of segments in the ring. The parameter β_n is also an integer. Once the VP for the ring has been determined and these trial functions substituted into it, the coefficients A_n, C_n and E_n can be determined using the standard Rayleigh-Ritz procedure (cf. A.L. Fetter and J.D. Walecka [Theoretical Mechanics of Particles and Continuous Media, McGraw-Hill, New York, pp. 219-244 (1980)]).

The shell is modeled in spherical coordinates (r, θ, ϕ). Since the shell surface has a constant radius of curvature, and assuming axisymmetric excitation, the trial functions depend on the azimuthal coordinate θ only. The choice of these particular basis functions for the shell displacements ensures that the motion of the shell at the crown ($\theta=0$) is purely radial, i.e. $u_t=0$, and that the resonance frequencies for a closed spherical shell predicted by the analytical solution of W.E. Baker [J. Acoust. Soc. Am. 33, pp. 1749-1758 (1961)] are reproduced exactly.

NUWC

IN-AIR COUPLING OF RING DRIVER AND SHELL

- PIEZOELECTRIC VARIATIONAL PRINCIPLE AND SHELL VARIATIONAL PRINCIPLE MUST BE SOLVED SIMULTANEOUSLY UNTIL CONVERGED RESULT FOR THE RESONANT FREQUENCY IS OBTAINED
- BOUNDARY CONDITIONS AT SHELL-DRIVER INTERFACE

$$w_0 \cos\theta_0 - u_0 \sin\theta_0 = u_{zp}$$

$$w_0 \sin\theta_0 + u_0 \cos\theta_0 = u_{rp}$$

$$M_\theta(\theta_0) = k^2 \left[\frac{\partial}{\partial\theta} + \nu \cot\theta_0\right]\left[\gamma u_0 + \frac{\partial w_0}{\partial\theta}\right] = 0$$

- ADDITIONAL BOUNDARY CONDITIONS
  - PURELY AXIAL SHELL MOTION AT CROWN
  - COMPRESSIVE PRE-STRESS ON OUTER RING SURFACE
  - STRESS-FREE ON INNER RING SURFACE
  - TOP AND BOTTOM RING SURFACES STRESS FREE AND ELECTRICALLY FREE

S3111-92.10.28-B1a

FIGURE 5

In order to model the ring-shell transducer in air, careful consideration must be given to the boundary conditions at the shell-driver interface. Of the greatest importance is matching the displacement of the ring driver with that of the shell at the point of intersection $\theta = \theta_0$. Furthermore, we have assumed that the bending moment M_θ of the shell at the shell-driver interface is zero. This may not be exactly correct, but the bending moment of the shell at this point is in all likelihood small enough to warrant such an approximation. Additional studies of the effect of various moment conditions on the results presented here will be carried out in the future. In addition to these interface conditions, several other boundary conditions must be satisfied. The trial functions for the shell are such that the motion of the shell at the crown (θ=0) is purely radial. The effect of the fiberglass wrapping is approximated by constraining the normal stress on the outer surface of the ring. The inner surface of the ring, on the other hand, is assumed to be stress-free. Furthermore, the top and bottom surfaces of the ring driver are assumed to obey mechanically stress-free and electrically free boundary conditions, except where the shell intersects the ring.

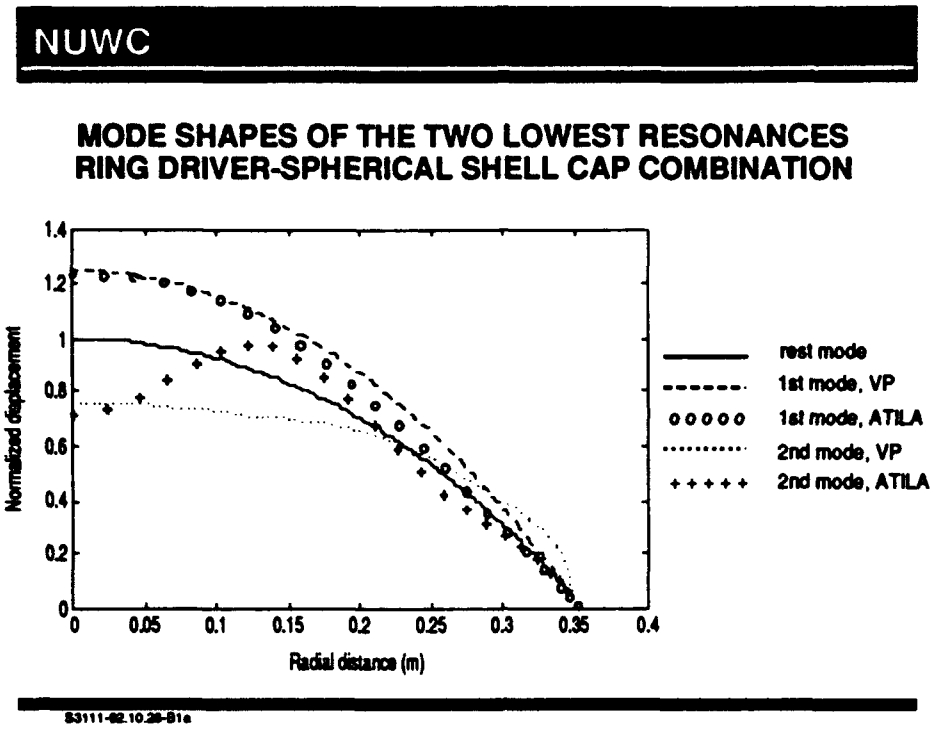

FIGURE 6

The in-air mode shapes of the ring-shell projector calculated variationally are compared with ATILA finite element results from J.B. Blottman ["Sparton Ring-Shell Single Element Modeling," NUSC Tech. Memo. No. 89-1090, 6 June 1989]. Only the shell displacement is shown here as a function of radial distance from the line $\theta=0$, since the ring moves very little. The actual displacements are exaggerated by a factor of 400 and are normalized to the rest position of the crown of the shell. As can be seen, the lowest variational resonant mode agrees quite well with the finite element prediction, with a maximum deviation of approximately 5%. This mode clearly is one in which the motion of the shell is purely normal to the shell surface, i.e. $u=0$ for this mode. The second mode, on the other hand, shows quite a bit of deviation from the finite element calculation. However, on comparison with the results presented in the Blottman study, it appears that the variationally determined mode shape for the second mode closely parallels the second antiresonance mode shape predicted by the finite element method. We can infer that the variational principle, as presently formulated, does not distinguish between the resonant and antiresonant modes, and simply chooses the one which is "simplest" as the correct solution. However, as we shall see, this deficiency does not appear to be a serious drawback, since it is the expression for the resonance frequency that is stationary with respect to variations in the mode shape and not vice versa. Apparently, the VP as formulated searches for an extremum rather than an absolute minimum.

NUWC

RESONANCE FREQUENCIES FOR RING-SHELL IN AIR

	RESONANCE FREQUENCIES (HZ)	
	1ST MODE	2ND MODE
VARIATIONAL PRINCIPLE	960	1345
ATILA	956.8	1331
EXPERIMENT(± 40 Hz)	920	1320

S3111-02.10.28-91a

FIGURE 7

The variationally calculated resonance frequencies of the ring-shell in air are compared to finite element and experimental values. The experimental in-air data was obtained under the NATO Comparative Test Program (CTP) by M. Werbicki ["In-Water Tests of the Sparton of Canada (SOC) Class V Flextensional Transducer," NUSC Tech. Memo. No. 901093, 29 May 1990], using a wide frequency sweep at 40 Hz increments and no tuning. The variational and ATILA results agree very well for the 1st mode, and both fall within the range of experimental error for this mode. For the second mode, both variational and finite element results fall within the error of the experimental data, with the finite element calculation coming somewhat closer to the "true" value of the resonance frequency. However, it must be noted that the variationally determined resonance frequency falls above both the resonance and antiresonance frequencies of the second mode determined by ATILA, lending further credence to the hypothesis that the VP for the ring-shell transducer does not discriminate between resonance and antiresonance modes. The important feature of these results is that, despite the fact that the variationally determined mode shapes may not be good representations of the actual transducer behavior, the resonance frequencies calculated using them are still within acceptable error limits.

Having completed and validated the in-air model of the ring-shell transducer, fluid loading effects must be incorporated to yield a workable transducer model. The remainder of this document will concentrate on this aspect of the analysis, and on the question of how accurate the in-air description must be in order to accurately model the transducer in water.

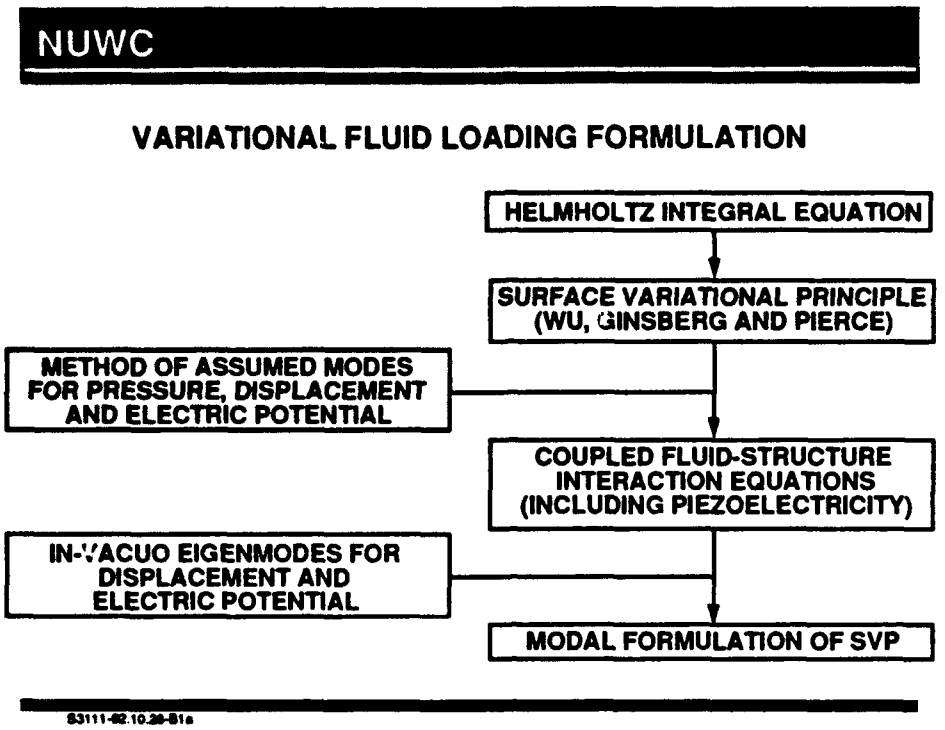

FIGURE 8

The variational formulation of fluid-loading effects begins with the familiar Helmholtz integral equation (c.f. M.C. Junger and D. Feit [Sound, Structures and Their Interaction, 2nd ed., MIT Press, Cambridge, MA (1986)]) relating the sound pressure in a fluid to the velocity and pressure distribution on the surface of a radiating body submerged in it. The Helmholtz integral involves free-field Green's functions which become singular as the source and field points approach one another. By allowing the field point to approach the surface gradually and carefully taking the limits of the integrals involved, X.F. Wu ["Variational Principles for Acoustic Radiation and Diffraction From Underwater Structures," Georgia Institute of Technology Rept. No. GTADL-TR-87-102, 24 November 1987] and J.H. Ginsberg, P.T. Chen and A.D. Pierce [J. Acoust. Soc. Am. 88, pp. 548-559 (1990)] developed a variational expression for the pressure on the surface of a radiating body with a prescribed surface velocity. Structural effects can be incorporated using the so-called method of assumed modes, e.g. assuming a basis function expansion for the pressure, displacement and electric potential of a flextensional transducer. This yields a set of coupled fluid-structure interaction equations for the transducer which are similar in form to the finite element formulation of R.R. Smith, J.T. Hunt, and D. Barach [J. Acoust. Soc. Am. 54, pp. 1277-1288 (1983)]. The critical difference here is that the structure has not been discretized in any way. The complexity of the problem may be further reduced by utilizing the in-vacuo eigenmodes for the displacement of the structure, leading to a modal formulation of the surface variational principle (SVP).

NUWC

FLUID LOADING IN RING-SHELL TRANSDUCER MODEL

- **EXPRESS DISPLACEMENTS AND ELECTRIC POTENTIAL IN TERMS OF IN-VACUO EIGENMODES OF RING-SHELL TRANSDUCER**

$$\vec{U}(\vec{x}) = \sum_{m=1}^{L} \eta_m \vec{U}_m(\vec{x}) \qquad \Phi(\vec{x}) = \sum_{m=1}^{L} \eta_m \phi_m(\vec{x})$$

- **TRIAL FUNCTIONS FOR SURFACE PRESSURE**

$$p(s) = \sum_{n=1}^{N_p} P_n \cos\left[\frac{(n-1)\pi}{S_{max}} s\right]$$

- **MODAL FORMULATION OF SVP**

$$\begin{bmatrix} [\omega_n^2 - \omega^2] & [\Lambda] \\ -[\Gamma] & [A] \end{bmatrix} \begin{bmatrix} \{\eta\} \\ \{P\} \end{bmatrix} = \begin{bmatrix} \{F_m\} \\ \{F_p\} \end{bmatrix}$$

83111-92.10.28-81a

FIGURE 9

The variationally determined eigenmodes of the transducer are denoted by $\vec{U}_m$ (for the combination of the shell and driver displacements) and by ϕ_m (for the electrostatic potential). Any arbitrary displacement and potential can now be expressed as a linear combination of these modes. This combination fully describes the structural and electrical transducer response. Since the ring-shell transducer is axisymmetric, the spatial coordinates of the surface may be described in terms of a generating parameter s, to be defined momentarily. The surface pressure on the transducer can now be written as an expansion of simplistic basis functions of the parameter s as indicated above. Combining these expansions with the coupled fluid-structure interaction equations yields the modal formulation of the surface variational principle (SVP), where $\{\eta\}$ and $\{P\}$ denote the set of expansion coefficients for the in-vacuo eigenmodes and the surface pressure, respectively. ω_n^2 is the in-vacuo resonance frequency of the transducer. The matrices $[\Lambda]$ and $[\Gamma]$ incorporate the coupling between the motion of transducer and the fluid. The matrix $[A]$ gives the pressure self-interaction contributions. $\{F_m\}$ and $\{F_p\}$ represent any external forcing functions. The solution of this matrix equation for a given frequency ω yields the variationally determined surface pressure of the radiating body. This surface pressure, together with prescribed surface velocity distribution, can then be utilized in the Helmholtz integral equation to calculate the far-field pressure.

NUWC

GENERATOR REPRESENTATION OF RING-SHELL TRANSDUCER

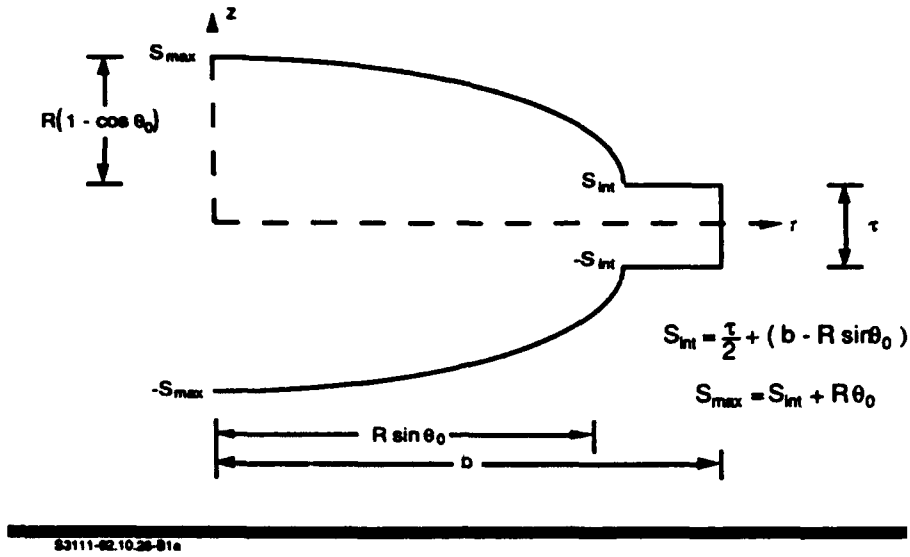

FIGURE 10

The axisymmetry of the ring-shell configuration is exploited by representing the surface of the transducer by the coordinates [r(s), z(s)], where s is a parameter measuring the length along the surface from the bottom crown of the shell, located at $s = -S_{max}$:

$$r(s) = \begin{cases} R\sin[(s + S_{max})/R] & -S_{max} \le s \le -S_{int} \\ (\tau/2 + b) + s & -S_{int} \le s \le -\tau/2 \\ b & -\tau/2 \le s \le \tau/2 \\ (\tau/2 + b) - s & \tau/2 \le s \le S_{int} \\ R\sin[(s - S_{max})/R] & S_{int} \le s \le S_{max} \end{cases}$$

$$z(s) = \begin{cases} -\tau/2 - R\{\sin[(s + S_{max})/R] - \cos\theta_0\} & -S_{max} \le s \le -S_{int} \\ -\tau/2 & -S_{int} \le s \le -\tau/2 \\ s & -\tau/2 \le s \le \tau/2 \\ \tau/2 & \tau/2 \le s \le S_{int} \\ \tau/2 + R\{\sin[(s + S_{max})/R] - \cos\theta_0\} & S_{int} \le s \le S_{max} \end{cases}$$

The origin s = 0 lies halfway up the outer surface of the ring driver, so that r (s = 0) = b and z (s = 0) = 0. Note that the intersection between the shell and the ring driver, S_{int}, is expressible purely in terms of the ring height τ, the outer radius b, the shell radius of curvature R, and the angle θ_0. S_{max} is given by adding S_{int} to the arc length of the shell. Rotation of this generator about the z axis gives the complete three-dimensional geometry for the surface of the transducer. All the pertinent physical quantities are expressible in terms of this generator parameter, and therefore all the calculations involve integrations over the parameter s only.

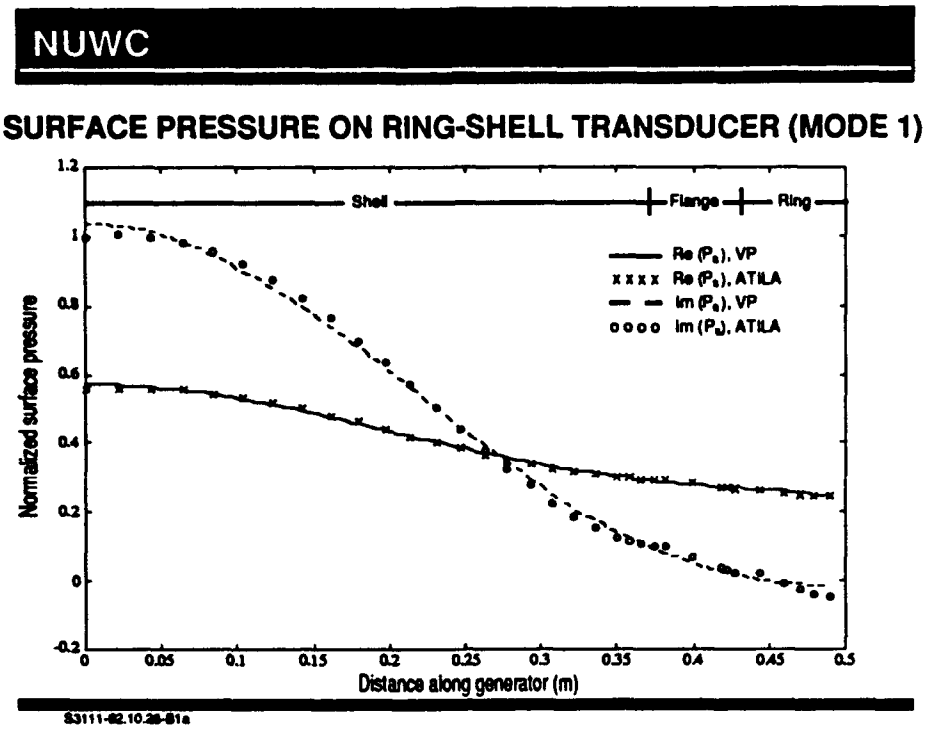

FIGURE 11

The variationally calculated surface pressure for a fluid-loaded ring-shell transducer is compared with the corresponding ATILA values for the first resonant mode (ca. 600 Hz) in the above figure. This variational calculation requires one in-vacuo eigenmode for the transducer structure and four surface pressure trial functions. The pressure has been normalized to the maximum value of the imaginary part of the surface pressure calculated using ATILA. The distance along the generator is measured from the crown of the shell to the midpoint of the outer radius of the ring. Since the transducer is symmetric about the midplane of the ring, the surface pressure is symmetric about that point as well. As can be seen, the surface pressures calculated variationally compare favorably with those calculated using finite elements. It is of interest to note that, despite the fact that the variational model does not include a flange, the general behavior of the surface pressure over the region where the flange would exist in reality is modeled well, although some of the finer details (i.e. local maxima and minima and pressure contour discontinuities associated with the corners of the flange and the flange-driver interface) are not represented. Nonetheless, it is evident that even using relatively unsophisticated trial functions for the surface pressure can yield very good results.

NUWC

SURFACE PRESSURE ON RING-SHELL TRANSDUCER (MODE 2)

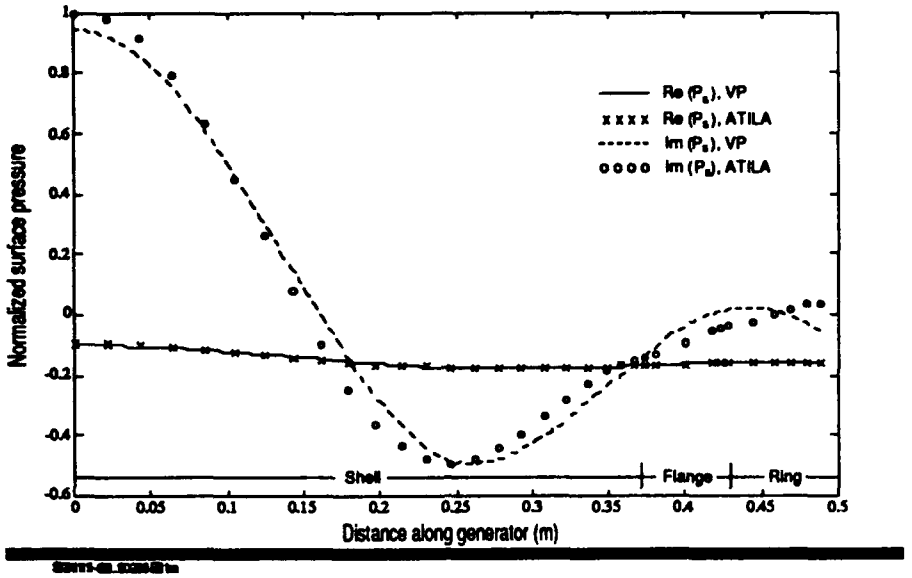

FIGURE 12

A comparison of variational and finite element results for the second resonant mode (ca. 1 KHz) is shown above. The agreement between the variational and ATILA results is somewhat worse than for the first mode. This is to be expected since, in general, variational formulations yield progressively worse results as one calculates higher eigenvalues. Nevertheless, the general behavior of the pressure on the shell is still shown by the variational calculations, and the discrepancy between the finite element and variational pressures is, at most, 5%. One interesting feature of this calculation is shown by the ring behavior. ATILA predicts, quite correctly, that the surface pressure over the outside surface of the ring driver will be nearly constant, since the displacement of the ring is almost purely radial and uniform. However, the surface pressure trial functions used in the variational calculations are not formulated to reflect this property, hence the digression in results. An improved trial function incorporating uniformity of the surface pressure over the outside surface of the ring would probably increase the accuracy of the variational results.

These surface pressures can now, in principle, be utilized to calculate the far-field pressures in two ways. For simple trial functions, the surface pressure distribution may be substituted back into the Helmholtz integral equation to obtain the far-field pressure. An alternative is to use spherical Hankel functions, which are the exact solution in the far-field, as trial functions and utilize the coefficients determined by the SVP to calculate the far-field directly. A drawback to this approach is that much of the flexibility in the variational formulation is lost.

NUWC

FLEXTENSIONAL TRANSDUCER MODELING USING VARIATIONAL PRINCIPLES--CONCLUDING REMARKS

- VARIATIONAL PRINCIPLES FOR PIEZOELECTRIC DRIVER AND SHELL ELEMENTS OF FLEXTENSIONAL TRANSDUCERS HAVE BEEN DEVELOPED AND VALIDATED
- COUPLING PIEZOELECTRIC AND SHELL ELEMENTS TO MODEL RING-SHELL TRANSDUCER IN AIR YIELDS GOOD RESULTS FOR RESONANCE FREQUENCIES
- INCLUDING FLUID LOADING USING SURFACE VARIATIONAL PRINCIPLE FORMULATION GIVES SURFACE PRESSURE VALUES IN GOOD AGREEMENT WITH FINITE ELEMENT PREDICTIONS
- IMPROVED TRIAL FUNCTIONS FOR THE SURFACE PRESSURE WILL IMPROVE RESULTS AND COULD LEAD TO BEAM PATTERNS WITHOUT FURTHER CALCULATION

FIGURE 13

In conclusion, it can be seen that the variational principle gives us yet another mathematical framework with which to analyze transducers. The variational principles for the resonance frequency of the driver, shell and transducer in-air have been shown to give very good results, even when using relatively unsophisticated trial functions. Inclusion of fluid-loading leads to the variational principle for the surface pressure, which yields surface pressures in good agreement with finite element predictions. These surface pressures can be used to calculate the far-field pressure using the Helmholtz integral equation. In addition, more rigorous expansions for the surface pressure, using the exact solutions for the pressure in the far-field, could be utilized to obtain the far-field beam pattern directly.

A brief word about computational efficiency is in order here. It is difficult to directly assess the relative computational speed of the variational method and the finite element code ATILA for several reasons. First, the variational calculations were done on the VEAMF1 (VAXvector 6510) machine using MATLAB software, whereas the ATILA runs were done on a Microvax. Thus, the operating systems and programming languages for the two analyses are considerably different. Secondly, and probably most importantly, the variational programs used in this analysis are, in their present form, not configured to run efficiently as a single package, but rather as a train of programs to be followed in sequence. Subsequent programming to streamline the variational computations should improve the efficiency considerably.

DISTRIBUTION LIST

EXTERNAL
ONR 451 (T. Goldsberry)
NRL/USRD, Orlando (J. Blue)
NCCOSC/DIV NRAD (D. Barach, G. Benthien)
NPS (S. Baker, D. Canright, C. Scandrett)
ARPA (W. Carey)
Bolt, Beranek and Newman, New London (B. Marshall)
University of Connecticut (Y. Hahn)
General Electric CR&D (R. Morrow)
Georgia Institute of Technology (J. Ginsberg, K. Wu)
Image Acoustics, Inc. (J. Butler, C. Sherman)
Lockheed/Sanders (R. Porzio)
Pennsylvania State University (W. Thompson)
Phonon Corp. (T. Martin)
Toko America (J. Gau)
Westinghouse Electric Corp., Naval Systems Division (M. Johnson)
British Aerospace (R. Oswin)
ISEN, France (J.-N. Decarpigny, B. Hamonic)
Universidad Nacional Del Sur, Argentina (P. Laura)